

RF operation of AlN/Al_{0.25}Ga_{0.75}N/AlN HEMTs with f_T/f_{max} of 67/166 GHz

Eungkyun Kim,^{1, a)} Jashan Singhal,^{1, b)} Austin Hickman,¹ Lei Li,¹ Reet Chaudhuri,¹ Yongjin Cho,¹ James C. M. Hwang,² Debdeep Jena,^{1, 2, 3} and Huili Grace Xing^{1, 2, 3}

¹⁾School of Electrical and Computer Engineering, Cornell University, Ithaca, New York 14853, USA

²⁾Department of Materials Science and Engineering, Cornell University, Ithaca, New York 14853, USA

³⁾Kavli Institute at Cornell for Nanoscale Science, Cornell University, Ithaca, New York 14853, USA

(Dated: 7 September 2023)

We report on highly-scaled Al_{0.25}Ga_{0.75}N channel high electron mobility transistors (HEMTs). Regrown ohmic contacts covering the sidewall of the compressively strained Al_{0.25}Ga_{0.75}N channel exhibited a low contact resistance of $R_c = 0.23 \Omega\cdot\text{mm}$. Scaled devices with a T-shaped gate showed record high speed for any AlGa_N-based transistors, $f_T/f_{max} = 67/166$ GHz, while simultaneously achieving high average breakdown field exceeding 2 MV/cm. The load-pull measurements performed at 10 GHz revealed a 20% peak power added efficiency (PAE) with an output power density of 2 W/mm, which is mainly limited by the RF dispersion. These results show promise for AlGa_N channel HEMTs as a candidate for the next generation RF power amplifier.

AlGa_N channel high electron mobility transistors show potential for next-generation high-power RF applications with the promise of a high Johnson's figure of merit ($JFOM = V_{br} \times f_T$) compared to the incumbent GaN HEMT technology¹⁻³. Therefore, it is critical to increase the device's three-terminal off-state breakdown voltage V_{br} while ensuring a high unit gain cutoff frequency f_T in order to achieve superior RF performance. Previous theoretical studies have suggested that the saturation velocity v_{sat} of AlGa_N alloys is comparable to GaN^{2,4,5}. This indicates that for equivalent device dimensions, the maximum achievable f_T^{max} in HEMTs, which is determined by the ratio of saturation velocity to gate length, should be similar for AlGa_N and GaN channels. With a higher breakdown field and similar saturation velocity, AlGa_N channel transistors are therefore expected to deliver higher power density at high frequencies.

While it might seem intuitive to maximize the Al content in the AlGa_N channel HEMTs for superior RF performance due to higher breakdown voltage, such consideration has to be balanced with other design concerns⁶. For example, when the Al content increases, the low-field mobilities and carrier densities in the AlGa_N channel decrease, increasing the sheet resistance and, as a result, the parasitic delay, thereby reducing f_T and f_{max} . Moreover, it becomes difficult to make ohmic contacts to the AlGa_N channel as the Al concentration of AlGa_N grows⁷⁻¹². So, an optimal Al mole fraction of the AlGa_N channel needs to be chosen that simultaneously maximizes f_T , f_{max} , and V_{br} to demonstrate an improvement over the conventional GaN HEMT technology.

Although AlGa_N-channel transistors are making rapid progress in long-channel devices designed for power-switching applications, there are limited reports of their RF performance. Xue *et al.*¹³ reported a record f_T/f_{max} of 40/58

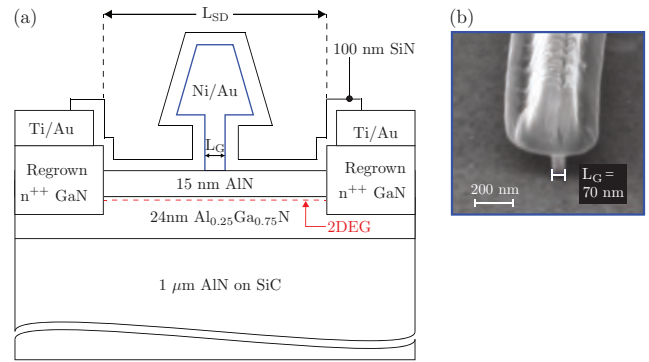


FIG. 1. (a) Cross-sectional representation of the fully processed AlN/Al_{0.25}Ga_{0.75}N/AlN HEMTs with a T-shaped gate. (b) SEM image of a 70 nm T-shaped gate cross section.

GHz for Al_{0.75}Ga_{0.25}N/Al_{0.6}Ga_{0.4}N HEMTs. The highest output power of Al-rich AlGa_N to date, 2.7 W/mm at 10 GHz albeit at a low PAE of 4%, was achieved in microchannel Al_{0.65}Ga_{0.35}N/Al_{0.4}Ga_{0.6}N HFET structures¹⁴.

In this study, we report a highly scaled T-gated Al_{0.25}Ga_{0.75}N quantum well channel HEMT (QW HEMT), for improved RF performance. We demonstrate devices with simultaneously high I_D^{max} (> 900 mA/mm) with low R_{on} ($= 6.5 \Omega\cdot\text{mm}$), high average breakdown field strength (> 2 MV/cm) and record-high $f_T/f_{max} = 67/166$ GHz for AlGa_N channel HEMTs. We demonstrate high average breakdown voltage without any field plate technique, which could potentially provide cost advantages for high-voltage RF applications.

The AlN/Al_{0.25}Ga_{0.75}N/AlN QW HEMTs presented in this study were grown on semi-insulating 6H-SiC substrates by plasma-assisted molecular beam epitaxy. The as-grown heterostructure consists of a 1 μm AlN buffer layer, a 24 nm Al_{0.25}Ga_{0.75}N channel, and a 15 nm AlN barrier. Further details on epitaxial growth are presented in Ref. 15. Nanomet-

^{a)}Electronic mail: ek543@cornell.edu

^{b)}Electronic mail: js3452@cornell.edu

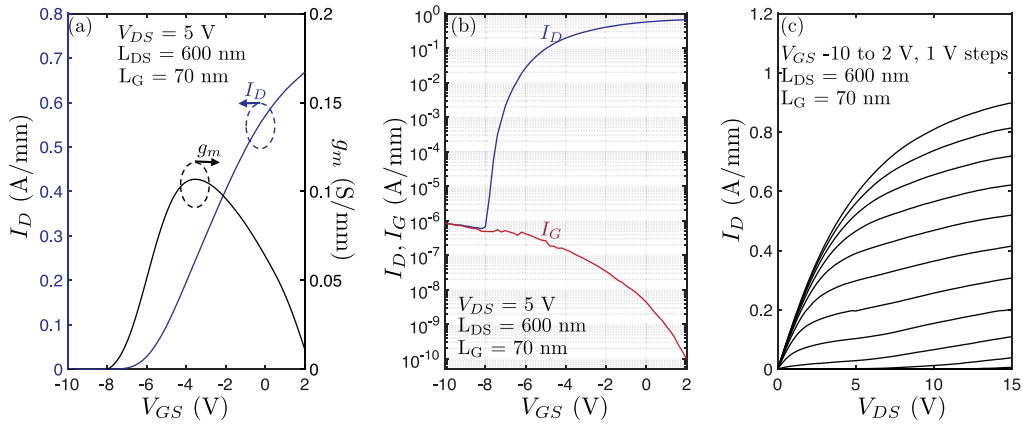


FIG. 2. DC characteristics of the AlN/Al_{0.25}Ga_{0.75}N/AlN HEMTs. The linear (a) and log (b) scale transfer characteristics, showing a peak transconductance of 0.11 S/mm and an on/off ratio exceeding 6 orders. (c) Output characteristics demonstrating a maximum drain current of 0.9 A/mm at a gate voltage of 2 V.

rics HL5500 Hall measurement system was used to characterize the as-grown sample. With soldered corner indium contacts to the 2DEG at the top AlN/AlGaN interface, a charge density and electron mobility of $3.05 \times 10^{13} \text{ cm}^{-2}$ and $45 \text{ cm}^2/\text{V}\cdot\text{s}$ were measured, respectively.

The fabrication process used for the QW HEMTs in this study is an extension of the process presented in Ref. 6. To explore the RF performance of AlN/AlGaN/AlN HEMTs, an electron beam lithography (EBL) defined T-shaped gate was introduced in place of a rectangular gate previously defined by photolithography, and a SiN passivation layer was added for an improved dispersion control. A tri-layer resist stack was patterned by EBL, and a Schottky contact was formed by sputtering 10 nm Ni and e-beam evaporating 300 nm Au. The HEMTs were then passivated with 100 nm plasma-enhanced chemical vapor deposition SiN. Figs. 1(a) and 1(b) show the final HEMT cross-section and a scanning electron microscope (SEM) image of a T-gate, respectively. The reported HEMTs feature a source-to-drain spacing $L_{SD} = 600 \text{ nm}$, $W_G = 2 \times 25 \mu\text{m}$ device width, and a T-shaped gate placed in the middle of the source-to-drain spacing with a gate length $L_G = 70 \text{ nm}$.

The DC characterization of the HEMTs was done using a Keithley 4200 parameter analyzer. After the device fabrication, a contact resistance from the top metal pad to 2DEG (R_c) and a sheet resistance (R_{sh}) were extracted by the linear transfer length method (TLM). The extracted $R_{sh} = 4.66 \text{ k}\Omega/\text{sq}$ closely matches with that measured on the as-grown sample via Hall-effect, indicating minimum process damage. The regrown n+ GaN non-alloyed ohmic contacts exhibited $R_c = 0.23 \Omega\cdot\text{mm}$, which is the lowest value among all Al-GaN channel HEMTs reported in the literature. Figs. 2(a) and (b) show the transfer curves measured at a drain bias $V_{DS} = 5 \text{ V}$, revealing an on/off ratio exceeding 10^6 with sharp pinch-off characteristics and a peak transconductance $g_m = 0.11 \text{ S/mm}$. The output curves in Fig. 2(c) show a maximum drain current $I_D = 0.9 \text{ A/mm}$ at a gate bias $V_{GS} = 2 \text{ V}$ and an on-resistance $R_{on} = 6.5 \Omega\cdot\text{mm}$. The observed DC output conductance (G_{DS}) is higher than that of previously re-

ported AlN/GaN/AlN HEMTs with a similar gate length^{16,17}, suggesting the presence of short channel effects (SCE). The cause of SCE is most likely a thicker AlN barrier used in this study, resulting in a low channel aspect ratio (L_G/d , d = gate-to-channel distance) less than 4.5^{18} . Further supported by negligible G_{DS} observed in AlGaIn channel HEMTs with a longer gate length on the same chip⁶, where we previously reported the details on the epitaxy and low-field transport in AlGaIn channel HEMT structures, the short channel effect is expected to be suppressed upon thinning down the top AlN barrier.

To investigate the dynamic and transient behavior, pulsed I-V measurements were performed using 4225-PMU modules with a Keithley 4200 parameter analyzer. 500 ns long pulses and a 1 ms period were used, and the drain current density at $V_{GS} = 0 \text{ V}$, -4 V , and -9 V was pulsed from different biasing conditions, $(V_{GSq}, V_{DSq}) = (0 \text{ V}, 0 \text{ V})$, $(-10 \text{ V}, 0 \text{ V})$, and $(-10 \text{ V}, 10 \text{ V})$, to assess current collapse and knee walkout. The AlGaIn channel HEMTs demonstrated appreciable RF dispersion, with an average of $\sim 10\%$ current collapse (shown in Fig. 3(a)). The possible sources of current dispersion include the surface states and a formation of a 2-dimensional hole gas or a filling of hole traps located near the valence band edge at the bottom GaN/AlN interface with a net negative polarization charge^{19,20}. To suppress RF dispersion in future devices, a proper control of surface states with an in-situ passivation layer and a Si- δ doping in the AlN back barrier to compensate positive charges may be necessary²¹.

RF characterization was performed using an Agilent 8722ES network analyzer and Infinity GSG probes. After the Short-Open-Load-Through calibration, scattering parameters were measured in the frequency range of 100 MHz to 40 GHz, and parasitic elements were de-embedded using on-wafer open and short structures. f_T and f_{max} were extracted from scattering parameters by extrapolating $|h_{21}|^2$ and a unilateral gain U , respectively, following the -20 dB/dec slope. As shown in Fig. 3(b), the HEMTs biased at $(V_{GS}, V_{DS}) = (-4 \text{ V}, 10 \text{ V})$ for maximum transconductance demonstrated a

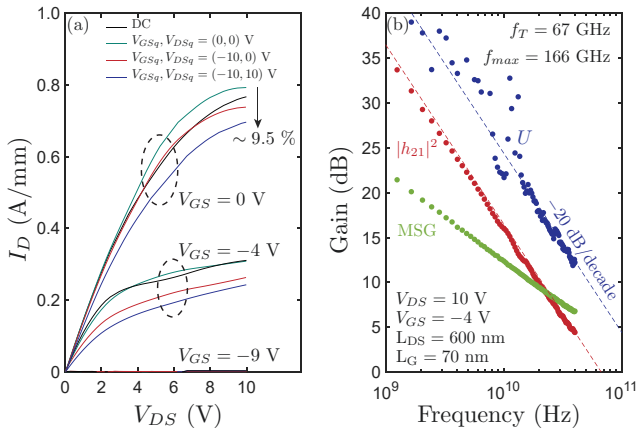


FIG. 3. (a) Pulsed $I_D V_D$ measured with a 500 ns pulsed with 0.05% duty cycle at different biasing conditions shown in the plot. Maximum current collapse of 10% and moderate knee walkout were observed. (b) Small signal characteristics of a HEMT with $L_G = 70$ nm, with an extrapolated $f_T/f_{max} = 67/166$ GHz at a gate and drain bias of -4 V and 10 V, respectively.

record-high $f_T/f_{max} = 67/166$ GHz for any AlGaIn channel HEMTs.

To explore the potential for high-frequency applications, sub-micron channel lengths were examined for breakdown. The three-terminal off-state breakdown voltage was measured by increasing V_{DS} until breakdown of the HEMT occurred with the gate voltage set below the threshold voltage, $V_{GS} \sim -10$ V. The breakdown voltage metric used in this study is defined as the drain voltage at which the drain current (I_D) exceeds 1 mA/mm. Fig. 4(a) shows the three terminal off-state breakdown of three AlGaIn QW channel HEMTs with varied gate-drain distances. Among all devices, a breakdown voltage of 59 V was measured for a HEMT with a 260 nm gate-drain distance. This corresponds to an average breakdown field exceeding 2 MV/cm. Fig. 4(b) shows the scaling of breakdown voltage as a function of L_{GD} , all the measured HEMTs show $E_{avg} > 1$ MV/cm, demonstrating the potential of QW HEMTs for extremely high-power operation in RF applications. It should be noted that, however, the devices examined for the breakdown characteristics are not free of dispersion as shown in Fig. 3(a). Unless properly passivated, the top barrier surface can become negatively charged by the electrons injected from the gate during off-state, extending the depletion width and lowering the peak electric field. Therefore, surface traps may be playing a role in increasing the breakdown voltage in measured devices. In order to accurately assess the impact of the AlGaIn channel on breakdown characteristics, careful control of surface states would be necessary in the future.

A Maury load-pull system at 10 GHz was used for large signal continuous wave RF measurements. After finding the impedance for maximum output power density (P_{out}) by tuning an external load, input power was swept to measure gain, P_{out} , and power-added efficiency (PAE). CW large signal load-pull measurement was performed at class AB operation with a bias condition of $V_{DS} = 15$ V and $V_{GS} = -3$ V. As shown in

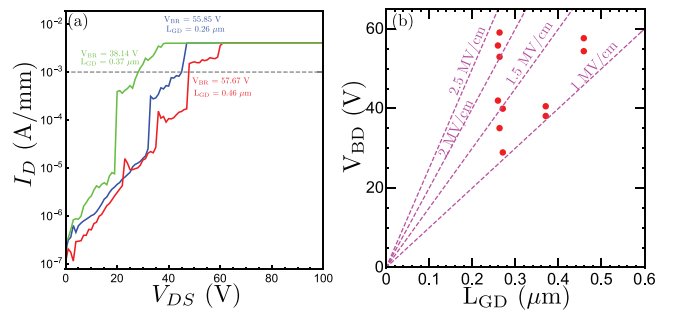


FIG. 4. Hard breakdown characteristics for three HEMTs with $L_{GD} = 0.26, 0.37,$ and 0.46 μm at a gate bias of -10 V. (b) Scaling of breakdown voltage as a function of L_{GD} .

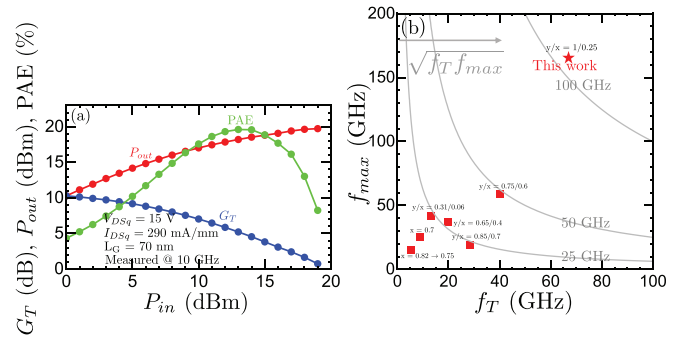


FIG. 5. (a) RF power sweep at 10 GHz at $V_{DSq}/V_{GSq} = 15/-3$ V, showing a peak PAE of 20% and maximum output power density of 2 W/mm. (b) Benchmark comparing f_T/f_{max} of AlGaIn channel HEMTs reported in the literature with this work. y/x indicates the Al composition in the top barrier/channel layer ($\text{Al}_y\text{Ga}_{1-y}\text{N}/\text{Al}_x\text{Ga}_{1-x}\text{N}$)^{13,14,22-25}.

Fig. 5(a), a saturation output power $P_{out} = 2$ W/mm is obtained at 10 GHz. The maximum PAE is measured to be $\sim 20\%$ and the power gain G_T is 5.2 dB at this condition. Further increase in PAE and P_{out} are limited by the soft gain compression, again attributed to the surface or bulk traps.

Lastly, in Fig. 5(b), the small signal characteristics are benchmarked in terms of f_T and f_{max} against the state-of-the-art AlGaIn channel HEMTs reported in the literature. In the benchmark plot, y and x indicate the Al mole fraction in the top barrier and the channel, respectively ($\text{Al}_y\text{Ga}_{1-y}\text{N}/\text{Al}_x\text{Ga}_{1-x}\text{N}$). The $\text{Al}_{0.25}\text{Ga}_{0.75}\text{N}/\text{AlN}$ QW HEMTs presented in this study exhibited the highest speed among all other AlGaIn channel transistors, with the record high f_T/f_{max} of 67/166 GHz. This translates to the geometric mean of f_T and f_{max} exceeding 105 GHz, breaking the 100 GHz barrier for the first time for AlGaIn channel HEMTs. The high speed observed in $\text{Al}_{0.25}\text{Ga}_{0.75}\text{N}$ channel HEMTs is attributed to a low contact resistance, which has been reported to be challenging to achieve with a higher Al composition AlGaIn channel, as well as an aggressively scaled gate length and source-to-drain distance. Although the electron mobility of AlGaIn channel HEMTs is lower (consequently R_{sh} is higher) than that of GaN channel HEMTs due to alloy scat-

tering, for RF devices the low mobility can be overcome by scaling the gate length to ensure that the carriers under the gate are velocity-saturated, while simultaneously reducing the source-to-drain distance to decrease the access resistance.

However, the contact resistance remains unaffected by the device scaling efforts due to the intrinsically lower electron affinity of a higher Al composition AlGa_N channel. This has led researchers to shift their focus from the conventional regrown n⁺-Ga_N contact method via MBE or MOCVD to exploring various contact formation schemes. Some of the highlights include $R_c = 0.43 \Omega\text{-mm}$ on Al_{0.5}Ga_{0.5}N using regrown n⁺-Ga_N prepared by pulsed sputtering deposition and $R_c = 4.3 \Omega\text{-mm}$ on Al_{0.64}Ga_{0.36}N using a Si-doped reverse graded Al_xGa_{1-x}N ($x = 0.87 \rightarrow 0.40$) layer^{26,27}. Despite the efforts, contact resistances reported in the literature for AlGa_N channel HEMTs with the Al mole fraction greater than 0.60 are still outside the acceptable range to outperform the Ga_N channel HEMTs for power amplification at high frequencies, highlighting the importance of ensuring low resistivity ohmic contacts. With proper scaling of devices, however, high Al composition AlGa_N channel HEMTs are expected to show a higher JFOM than that reported in this study with a relatively low Al composition, once the challenges in ohmic contact formation are addressed.

In summary, highly scaled Al_{0.25}Ga_{0.75}N quantum well channel HEMTs were demonstrated, showing a maximum drain current over 0.9 A/mm, a peak transconductance of 0.11 S/mm, and a record high speed $f_T/f_{max} = 67/166$ GHz. Devices with $L_{GD} = 270$ nm exhibited an average breakdown field exceeding 2 MV/cm and a maximum output power density of 2 W/mm with a 20% PAE in the X-band, where the output power is mainly limited by the soft gain compression. This initial set of data suggests that AlGa_N channel transistors can achieve a comparable level of gain at high frequencies to Ga_N channel transistors despite the lower electron mobility. This provides a clear path for transitioning into higher Al composition AlGa_N channel, provided that low resistivity ohmic contacts can be ensured.

ACKNOWLEDGMENTS

This work is supported by ULTRA, an Energy Frontier Research Center funded by the U.S. Department of Energy (DOE), Office of Science, Basic Energy Sciences (BES), under Award No. DE-SC0021230; AFOSR Grant No. FA9550-20-1-0148; and Semiconductor Research Corporation (SRC) Joint University Microelectronics Program (JUMP). This work uses the Cornell Nanoscale Facilities, supported by NSF grant NNCI-202523 and CESI Shared Facilities partly sponsored by NSF No. MRI DMR-1631282 and Kavli Institute at Cornell (KIC).

AUTHOR CONTRIBUTIONS

E.K. and J.S. contributed equally to this work.

DATA AVAILABILITY STATEMENT

The data that support the findings of this study are available from the corresponding author upon reasonable request.

- ¹J. Y. Tsao, S. Chowdhury, M. A. Hollis, D. Jena, N. M. Johnson, K. A. Jones, R. J. Kaplar, S. Rajan, C. G. Van de Walle, E. Bellotti, C. L. Chua, R. Collazo, M. E. Coltrin, J. A. Cooper, K. R. Evans, S. Graham, T. A. Grotjohn, E. R. Heller, M. Higashiwaki, M. S. Islam, P. W. Juodawlkis, M. A. Khan, A. D. Koehler, J. H. Leach, U. K. Mishra, R. J. Nemanich, R. C. N. Pilawa-Podgurski, J. B. Shealy, Z. Sitar, M. J. Tadjer, A. F. Witulski, M. Wraback, and J. A. Simmons, "Ultrawide-Bandgap Semiconductors: Research Opportunities and Challenges," *Advanced Electronic Materials* **4**, 1600501 (2018).
- ²A. G. Baca, A. M. Armstrong, B. A. Klein, A. A. Allerman, E. A. Douglas, and R. J. Kaplar, "Al-rich AlGa_N based transistors," *Journal of Vacuum Science & Technology A: Vacuum, Surfaces, and Films* **38**, 020803 (2020).
- ³M. E. Coltrin, A. G. Baca, and R. J. Kaplar, "Analysis of 2d transport and performance characteristics for lateral power devices based on algan alloys," *ECS Journal of Solid State Science and Technology* **6**, S3114 (2017).
- ⁴M. Farahmand, C. Garetto, E. Bellotti, K. Brennan, M. Goano, E. Ghillino, G. Ghione, J. Albrecht, and P. Ruden, "Monte carlo simulation of electron transport in the iii-nitride wurtzite phase materials system: binaries and ternaries," *IEEE Transactions on Electron Devices* **48**, 535–542 (2001).
- ⁵B. A. Klein, A. G. Baca, S. M. Lepkowski, C. D. Nordquist, J. R. Wendt, A. A. Allerman, A. M. Armstrong, E. A. Douglas, V. M. Abate, and R. J. Kaplar, "Saturation velocity measurement of al0.7ga0.3n-channel high electron mobility transistors," *Journal of Electronic Materials* **48** (2019), 10.1007/s11664-019-07421-1.
- ⁶J. Singhal, E. Kim, A. Hickman, R. Chaudhuri, Y. Cho, H. G. Xing, and D. Jena, "AlN/AlGa_N/AlN quantum well channel HEMTs," *Applied Physics Letters* **122**, 222106 (2023), https://pubs.aip.org/aip/apl/article-pdf/doi/10.1063/5.0145582/17936317/222106_1_5.0145582.pdf.
- ⁷E. A. Douglas, S. Reza, C. Sanchez, D. Koleske, A. Allerman, B. Klein, A. M. Armstrong, R. J. Kaplar, and A. G. Baca, "Ohmic contacts to al-rich algan heterostructures," *physica status solidi (a)* **214**, 1600842 (2017), <https://onlinelibrary.wiley.com/doi/pdf/10.1002/pssa.201600842>.
- ⁸T. Nanjo, M. Takeuchi, M. Suita, Y. Abe, T. Oishi, Y. Tokuda, and Y. Aoyagi, "First Operation of AlGa_N Channel High Electron Mobility Transistors," *Applied Physics Express* **1**, 011101 (2007).
- ⁹N. Yafune, S. Hashimoto, K. Akita, Y. Yamamoto, H. Tokuda, and M. Kuzuhara, "AlN/AlGa_N HEMTs on AlN substrate for stable high-temperature operation," *Electronics Letters* **50**, 211–212 (2014), <https://ietresearch.onlinelibrary.wiley.com/doi/pdf/10.1049/el.2013.2846>.
- ¹⁰S. Bajaj, F. Akyol, S. Krishnamoorthy, Y. Zhang, and S. Rajan, "AlGa_N channel field effect transistors with graded heterostructure ohmic contacts," *Applied Physics Letters* **109**, 133508 (2016), <https://doi.org/10.1063/1.4963860>.
- ¹¹S. P. Grabowski, M. Schneider, H. Nienhaus, W. Mönch, R. Dimitrov, O. Ambacher, and M. Stutzmann, "Electron affinity of Al_xGa_{1-x}N(0001) surfaces," *Applied Physics Letters* **78**, 2503–2505 (2001), <https://doi.org/10.1063/1.1367275>.
- ¹²I. Abid, J. Mehta, Y. Cordier, J. Derluyn, S. Degroote, H. Miyake, and F. Medjdoub, "AlGa_N Channel High Electron Mobility Transistors with Regrown Ohmic Contacts," *Electronics* **10** (2021), 10.3390/electronics10060635.
- ¹³H. Xue, C. H. Lee, K. Hussain, T. Razzak, M. Abdullah, Z. Xia, S. H. Sohel, A. Khan, S. Rajan, and W. Lu, "Al_{0.75}Ga_{0.25}N/Al_{0.6}Ga_{0.4}N heterojunction field effect transistor with f_T of 40 GHz," *Applied Physics Express* **12**, 066502 (2019).
- ¹⁴H. Xue, K. Hussain, T. Razzak, M. Gaevski, S. H. Sohel, S. Mollah, V. Tale-sara, A. Khan, S. Rajan, and W. Lu, "Al_{0.65}Ga_{0.35}N/Al_{0.4}Ga_{0.6}N Micro-Channel Heterojunction Field Effect Transistors With Current Density Over 900 mA/mm," *IEEE Electron Device Letters* **41**, 677–680 (2020).
- ¹⁵J. Singhal, R. Chaudhuri, A. Hickman, V. Protasenko, H. G. Xing, and D. Jena, "Toward AlGa_N channel HEMTs on AlN: Polarization-induced 2DEGs in AlN/AlGa_N/AlN heterostructures," *APL Materials* **10**, 111120 (2022), <https://doi.org/10.1063/5.0121195>.

- ¹⁶A. Hickman, R. Chaudhuri, S. J. Bader, K. Nomoto, K. Lee, H. G. Xing, and D. Jena, "High breakdown voltage in RF AlN/GaN/AlN quantum well HEMTs," *IEEE Electron Device Letters* **40**, 1293–1296 (2019).
- ¹⁷A. Hickman, R. Chaudhuri, L. Li, K. Nomoto, S. J. Bader, J. C. Hwang, H. G. Xing, and D. Jena, "First RF power operation of AlN/GaN/AlN HEMTs with > 3 A/mm and 3 W/mm at 10 GHz," *IEEE Journal of the Electron Devices Society* **9**, 121–124 (2020).
- ¹⁸K. Shinohara, D. C. Regan, Y. Tang, A. L. Corrion, D. F. Brown, J. C. Wong, J. F. Robinson, H. H. Fung, A. Schmitz, T. C. Oh, S. J. Kim, P. S. Chen, R. G. Nagele, A. D. Margomenos, and M. Micovic, "Scaling of gan hemts and schottky diodes for submillimeter-wave mmic applications," *IEEE Transactions on Electron Devices* **60**, 2982–2996 (2013).
- ¹⁹M. B. Tahhan, J. A. Logan, M. T. Hardy, M. G. Ancona, B. Schultz, B. Appleton, T. Kazior, D. J. Meyer, and E. M. Chumbes, "Passivation schemes for scaln-barrier mm-wave high electron mobility transistors," *IEEE Transactions on Electron Devices* **69**, 962–967 (2022).
- ²⁰M. H. Wong, U. Singiseti, J. Lu, J. S. Speck, and U. K. Mishra, "Anomalous output conductance in n-polar gan high electron mobility transistors," *IEEE Transactions on Electron Devices* **59**, 2988–2995 (2012).
- ²¹R. Chaudhuri, A. Hickman, J. Singhal, J. Casamento, H. G. Xing, and D. Jena, "In situ crystalline aln passivation for reduced rf dispersion in strained-channel aln/gan/aln high-electron-mobility transistors," *physica status solidi (a)* **219**, 2100452 (2022), <https://onlinelibrary.wiley.com/doi/pdf/10.1002/pssa.202100452>.
- ²²T. Razzak, S. Hwang, A. Coleman, S. Bajaj, H. Xue, Y. Zhang, Z. Jamal-Eddine, S. Soheli, W. Lu, A. Khan, and S. Rajan, "Rf operation in graded alxga1xn ($x = 0.65$ to 0.82) channel transistors," *Electronics Letters* **54**, 1351–1353 (2018), <https://ietresearch.onlinelibrary.wiley.com/doi/pdf/10.1049/el.2018.6897>.
- ²³A. Raman, S. Dasgupta, S. Rajan, J. S. Speck, and U. K. Mishra, "Algan channel high electron mobility transistors: Device performance and power-switching figure of merit," *Japanese Journal of Applied Physics* **47**, 3359 (2008).
- ²⁴A. G. Baca, B. A. Klein, J. R. Wendt, S. M. Lepkowski, C. D. Nordquist, A. M. Armstrong, A. A. Allerman, E. A. Douglas, and R. J. Kaplar, "RF Performance of Al_{0.85}Ga_{0.15}N/Al_{0.70}Ga_{0.30}N High Electron Mobility Transistors With 80-nm Gates," *IEEE Electron Device Letters* **40**, 17–20 (2019).
- ²⁵H. Xue, T. Razzak, S. Hwang, A. Coleman, S. Bajaj, Y. Zhang, Z. Jamal-Eddin, S. H. Soheli, A. Khan, S. Rajan, and W. Lu, "All moccvd grown 250 nm gate length al_{0.70}ga_{0.30}n mesfets," in *2018 76th Device Research Conference (DRC)* (2018) pp. 1–2.
- ²⁶R. Maeda, K. Ueno, A. Kobayashi, and H. Fujioka, "AlN/Al_{0.5}Ga_{0.5}N HEMTs with heavily Si-doped degenerate GaN contacts prepared via pulsed sputtering," *Applied Physics Express* **15**, 031002 (2022).
- ²⁷A. Mamun, K. Hussain, R. Floyd, M. D. Alam, M. Chandrashekar, G. Simin, and A. Khan, "Al_{0.64}Ga_{0.36}N channel MOSFET on single crystal bulk AlN substrate," *Applied Physics Express* **16**, 061001 (2023).